

Department
of
APPLIED MATHEMATICS

A total pressure-saturation formulation of two-phase flow incorporating dynamic effects in the capillary-pressure-saturation relationship.

by

H. K. Dahle, M. A. Celia, S. Majid Hassanizadeh,
K. Hvistendahl Karlsen.

Report no. 166

January 2002



UNIVERSITY OF BERGEN
Bergen, Norway

Department of Mathematics
University of Bergen
5008 Bergen
Norway

ISSN 0084-778X

A total pressure-saturation formulation of two-phase
flow incorporating dynamic effects in the
capillary-pressure-saturation relationship.

by

H. K. Dahle ^a, M. A. Celia ^b, S. Majid Hassanizadeh ^c,
K. Hvistendahl Karlsen ^a.

^a Department of Mathematics, University of Bergen,
Johs. Brunsgt. 12, N-5008 Bergen, Norway

^b Department of Civil and Environmental Engineering
Princeton University
Princeton, NJ 08544, USA

^c Faculty of Civil Engineering and Geosciences
Delft University of Technology
P.O. Box 5084; 2600GA, Delft, The Netherlands

Report no. 166

NB Rana
Depotbiblioteket

January 2002

A total pressure-saturation formulation of two-phase flow incorporating dynamic effects in the capillary-pressure-saturation relationship.

H. K. Dahle^a M. A. Celia^b S. Majid Hassanizadeh^c K. Hvistendahl Karlsen^a,

^aDepartment of Mathematics, University of Bergen,
Johs. Brunsgt. 12, N-5008 Bergen, Norway

^bDepartment of Civil and Environmental Engineering
Princeton University
Princeton, NJ 08544, USA

^cFaculty of Civil Engineering and Geosciences
Delft University of Technology
P.O. Box 5084; 2600GA Delft; The Netherlands

New theories suggest that the relationship between capillary pressure and saturation should be enhanced by a dynamic term that is proportional to the time rate of change of saturation. This so-called dynamic capillary pressure formulation is supported by laboratory experiments, and can be included in various forms of the governing equations for two-phase flow in porous media. An extended model of two-phase flow in porous media may be developed based on fractional flow curves and a total pressure - saturation description that includes the dynamic capillary pressure terms. A dimensionless form of the resulting equation set provides an ideal tool to study the relative importance of the dynamic capillary pressure effect. This equation provides a rich set of mathematical research questions, and numerical solutions to the equation provide insights into the behavior of two-phase immiscible flow. For typical two-phase flow systems, dynamic capillary pressure acts to retard infiltration fronts, with responses dependent on system parameters including boundary conditions.

1. INTRODUCTION

Recent theoretical work, e.g. [7,8], suggests that the traditional algebraic relationship between capillary pressure and saturation may be inadequate. Instead, a so-called dynamic capillary pressure formulation is needed, where capillary pressure is defined as a thermodynamic variable, and the difference between phase pressures is only equal to the capillary pressure at equilibrium. Under dynamic conditions, the disequilibrium between phase-pressure differences and the capillary pressure is taken to be proportional to the time rate of change of saturation. A recent study by Hassanizadeh et al. [10] presents experimental evidence, culled from the literature, to support this claim. Numerical simulations using dynamic pore-scale network models, e.g. [5], and upscaling also support the claim. In [10], numerical solutions were presented for an enhanced version of Richards'

equation that included the dynamic terms. A preliminary assessment was made regarding the magnitude of the proportionality coefficient in the dynamic equation, identifying ranges that produce significant modification to infiltration results.

While the work presented in [10] provides a foundation for this problem, it only considered the specific case of flow in unsaturated soils, under the assumption that the air phase remains at essentially atmospheric pressure everywhere in the domain. In the present work, we expand this earlier work to include the general two-phase flow case, using a fractional flow formulation for the governing equations. Into these equations are embedded the dynamic capillary pressure terms. The equations are then written in dimensionless form, and a brief discussion of the mathematical properties of the enhanced governing equations is presented. A numerical algorithm for their solution is given, and a numerical simulation is presented to demonstrate the effects of the dynamic terms. Finally the implication of these results is discussed, and a few comments on future directions for research are given.

2. A TOTAL VELOCITY/GLOBAL PRESSURE FORMULATION

The basic equations describing two-phase immiscible flow in a porous medium are given by mass balance equations, Darcy's law, and associated constitutive relationships. In this section we present a total velocity-global pressure formulation, [4,3], including a dynamic capillary pressure term. Let $\Omega \subset \mathbf{R}^3$ denote the porous medium. Mass balance and Darcy's law for the phases are:

$$\frac{\partial \phi \rho_\alpha s_\alpha}{\partial t} + \nabla \cdot (\rho_\alpha u_\alpha) = q_\alpha, \quad x \in \Omega, \quad t > 0, \quad \alpha = w, n, \quad (1)$$

$$u_\alpha = -\lambda_\alpha K \cdot (\nabla p_\alpha - \rho_\alpha g \nabla z), \quad x \in \Omega, \quad t > 0, \quad \alpha = w, n. \quad (2)$$

Here, $\alpha = w, n$, denote the wetting and non-wetting phases, respectively; s_α, p_α , and ρ_α are the saturation, pressure and fluid density of phase α ; $\lambda_\alpha = k_{r\alpha}/\mu_\alpha$ is the mobility of phase α with $k_{r\alpha}$ and μ_α being the relative permeability and viscosity of the phase; q_α denotes a source term (mass per unit volume per time); ϕ is the effective porosity; K is the intrinsic permeability tensor; g is the gravity constant and z denotes the depth. In addition $\sum_\alpha s_\alpha = 1$, and we assume a *dynamic* relationship between pressures and saturations as derived by Hassanizadeh and Gray [8]:

$$p_n - p_w = P_c - L \frac{\partial s_w}{\partial t}. \quad (3)$$

Finally, we assume that

$$\lambda_\alpha = \lambda_\alpha(s_w), \quad P_c = P_c(s_w) \quad \text{and} \quad L = L(s_w) \geq 0. \quad (4)$$

The pressure difference giving the left-hand side of Equation (3) should be interpreted as a *dynamic* capillary pressure, whereas the P_c function on the right-hand side is the capillary pressure measured under *equilibrium* conditions. Subsequently we assume that L is constant, although results reported in [10] may suggest a more general behavior. Also note that the dimension of L is *mass/(length \times time)*. Next, we introduce

$$\lambda_T = \sum_\alpha \lambda_\alpha, \quad u = \sum_\alpha u_\alpha, \quad f_\alpha(s_\alpha) = \frac{\lambda_\alpha}{\lambda_T}, \quad \text{and} \quad d(s_\alpha) = \frac{\lambda_w \lambda_n}{\lambda_T}.$$

Here, λ_T is the total mobility, u is the total Darcy velocity, f_α is the fractional flow of phase α , and d is the harmonic average of the mobility functions. Define compressibilities $c_\alpha = (d\rho_\alpha/dp)/\rho_\alpha$ and $c_s = (d\phi/dp)/\phi$, and a global pressure by

$$p = h_w p_w + h_n p_n + \frac{1}{2} \{ (h_w - h_n) P_c - \int^{s_w} (f_w - f_n) P'_c d\xi \}. \quad (5)$$

Here the weights h_α , are assumed to be functions of s_w and sum to 1. With these definitions we can combine equations (1)-(3) to obtain:

$$\nabla \cdot u = -\phi c_s \frac{\partial p}{\partial t} - \sum_\alpha c_\alpha (\phi s_\alpha \frac{\partial p}{\partial t} + u_\alpha \cdot \nabla p) + \sum_\alpha q_\alpha / \rho_\alpha, \quad (6)$$

$$u = -\lambda_T K \cdot [\nabla p + \frac{1}{2} \{ (f_w - f_n) \nabla (L \frac{\partial s_w}{\partial t}) - \nabla ((h_w - h_n) L \frac{\partial s_w}{\partial t}) \} - (\lambda_w \rho_w + \lambda_n \rho_n) g \nabla z], \quad (7)$$

$$\begin{aligned} & \phi \frac{\partial s_w}{\partial t} + \nabla \cdot \{ f_w u + dK \cdot [(\rho_w - \rho_n) g \nabla z + \nabla (P_c - L \frac{\partial s_w}{\partial t})] \} \\ & = q_w / \rho_w - \phi s_w c_s \frac{\partial p}{\partial t} - c_\alpha (\phi s_w \frac{\partial p}{\partial t} + u_w \cdot \nabla p). \end{aligned} \quad (8)$$

Supplied with appropriate constitutive relationship, equations (6)-(8) form a closed set of equations with p and s_w as primary variables.

2.1. One dimensional model

Assume that the flow takes place in one spatial dimension such that $\Omega = (0, l) \in \mathbf{R}$. To simplify even more, assume that the flow is horizontal, $\nabla z = 0$, and that $c_s = c_\alpha = q_\alpha = 0$. Then equations (6)-(8) reduce to:

$$\frac{\partial u}{\partial x} = 0, \quad (9)$$

$$u = -\lambda_T K \left(\frac{\partial p}{\partial x} + \frac{1}{2} \{ (f_w - f_n) \frac{\partial}{\partial x} (L \frac{\partial s_w}{\partial t}) - \frac{\partial}{\partial x} [(h_w - h_n) L \frac{\partial s_w}{\partial t}] \} \right), \quad (10)$$

$$\phi \frac{\partial s_w}{\partial t} + \frac{\partial}{\partial x} \{ f_w u + dK \frac{\partial}{\partial x} (P_c - L \frac{\partial s_w}{\partial t}) \} = 0. \quad (11)$$

Equation (9) implies that $u = u(t)$. We can therefore integrate (10) in space to obtain:

$$u(t) = - \frac{p(l, t) - p(0, t) + \int_0^l \frac{1}{2} \{ (f_w - f_n) \frac{\partial}{\partial x} (L \frac{\partial s_w}{\partial t}) - \frac{\partial}{\partial x} [(h_w - h_n) L \frac{\partial s_w}{\partial t}] \} dx}{\int_0^l (K \lambda)_T^{-1} dx}. \quad (12)$$

This model is often used to describe core-plug experiments. To be able to solve (11) and (12) we need to specify the initial saturation $s_w(x, 0) = s_0(x)$ and appropriate boundary conditions. If the volumetric flux $u_\alpha = u_\alpha(t)$ of each phase is specified at the boundary, Equation (12) become redundant, and a total-flux condition may be imposed on the saturation equation (11). Furthermore, it is useful to write (11) in non-dimensional form:

$$\frac{\partial s}{\partial t} + \frac{\partial}{\partial x} \{ f_w(s) v(t) - a(s, x) [\epsilon b(s) \frac{\partial s}{\partial x} + \nu \frac{\partial^2 s}{\partial x \partial t}] \} = 0. \quad (13)$$

Here, l and \tilde{u} are respectively characteristic length scale and flow-rate; $\tilde{t} = l\phi(1 - s_{n_r} - s_{w_r})/\tilde{u}$ is the characteristic time scale; $s = (s_w - s_{w_r})/(1 - s_{n_r} - s_{w_r})$ is the reduced saturation; \tilde{P}'_c and \tilde{K} are characteristic values for $P'_c(s)$ and K ; $k_\alpha < 1$ are the end-point relative permeabilities; $\tilde{\lambda}_\alpha = \tilde{k}_\alpha/\mu_\alpha$; $\tilde{d} = \tilde{k}_w/\mu_w$. Dimensionless quantities are:

$$\kappa = \frac{\tilde{\lambda}_n}{\tilde{\lambda}_w}; \quad \epsilon = \frac{\tilde{d}\tilde{K}|\tilde{P}'_c|(1 - s_{n_r} - s_{w_r})}{\tilde{u}l}; \quad \nu = \frac{\tilde{d}\tilde{K}}{\phi l^2}L; \quad v(t) = \frac{u(t)}{\tilde{u}}; \quad \bar{\lambda}_\alpha(s) = \frac{\lambda_\alpha(s)}{\tilde{\lambda}_\alpha};$$

$$f_w(s) = \frac{\bar{\lambda}_w(s)}{\bar{\lambda}_w(s) + \kappa\bar{\lambda}_n(s)}; \quad a(s, x) = \frac{\kappa\bar{\lambda}_w(s)\bar{\lambda}_n(s)}{\bar{\lambda}_w(s) + \kappa\bar{\lambda}_n(s)} \cdot \frac{K(x)}{\tilde{K}}; \quad b(s) = -\frac{1}{|\tilde{P}'_c|}P'_c(s).$$

Notice that the Richards' equation including a dynamic term is formally obtained from (13) by letting $\kappa \rightarrow \infty$.

2.2. Sobolev equations

Except for the x and t dependency in coefficients, Equation (13) can be written in the generic form

$$u_t + f(u)_x = \epsilon g(u)_{xx} + \nu (h(u)u_{tx})_x, \quad (14)$$

where $u(x, t)$ is the solution that is sought; subscripts connote partial differentiation; $f(u)$ (convection), $g(u)$ (diffusion), and $h(u)$ (dispersion) are given functions; while $\epsilon, \nu > 0$ are given scaling parameters indicating the importance of diffusion (ϵ) and dispersion (ν). PDEs of the form (14), which often are referred to as *Sobolev equations* in the literature, occur in several different applications, besides the one considered herein. We mention briefly flow of fluids through fissured rocks, heat conduction, shear in second order fluids, and consolidation of clay (see also discussion below). It is worth while noticing that the time derivative of the solution to a Sobolev equation (14) is not given explicitly, and, for this reason, Sobolev equations are often also referred to as *implicit evolution equations*. Sobolev equations have been extensively studied in the literature, at least when the functions $g'(u)$ and $h(u)$ are bounded away from zero (the non-degenerate case). Unfortunately, in the applications considered herein the functions $g'(u), h(u)$ may both vanish for some solution values. A general mathematical theory (encompassing non-smooth solutions) for degenerate Sobolev equations of the type (14) has yet to be developed. Although a general theory is missing, a traveling wave analysis is carried out in [11] when $f \equiv 0$ (more precisely, the authors consider a Richard type equation). In the non-degenerate case, well-posedness of Sobolev equations are well-known. Typically, existence and uniqueness of solutions are established by using "abstract" Hilbert space techniques for evolution equations; see, e.g, [13] for some typical results and proofs. Let us also mention that Sobolev equations have been extensively analyzed from a numerical point of view, in particular when the convection term f is not dominating, see, e.g., [6] and the references therein for some classical papers on finite difference and finite element methods. Much more recently, in [9] the method of characteristics was applied to Sobolev equations with a dominating convection term. The finite difference scheme that we used herein (for the convection dominated regime) is in the spirit of the ones used in [12].

2.3. Vanishing diffusion-dispersion limits

Motivated by our numerical examples and the fact that we are particularly interested in the Sobolev equation (14) when convection effects dominates over diffusion/dispersion

effects, it is of great interest to understand the singular limit of solutions $u^{\nu,\mu}$ of (14) as $\epsilon, \nu \rightarrow 0$. Note that such a study is highly relevant when it comes to constructing correct and accurate numerical methods for convection dominated Sobolev equations. We can view (14) as a *diffusion-dispersion regularization* of the conservation law

$$u_t + f(u)_x = 0. \quad (15)$$

Currently there is no theory for the “ $\epsilon, \nu \rightarrow 0$ limit” of (14) when the dispersion coefficient $h(u)$ is a nonlinear function. However, theory is available for the Cauchy problem for a simpler Sobolev equation with a “constant dispersion coefficient”:

$$u_t + f(u)_x = \epsilon g(u)_{xx} + \nu u_{txx} \iff (1 - \nu \partial_x^2)u_t + f(u)_x = \epsilon g(u)_{xx}. \quad (16)$$

A particular example of this equation has been used to model the propagation of small amplitude shallow-water waves (as an alternative to the Korteweg-de Vries (KdV) equation), see [1]. For some recent results on (16) when $\epsilon = 0$ (in which case the equation possesses solitary-wave solutions), see [2].

3. NUMERICAL SOLUTION

To solve Equation (13) numerically, we shall use a semi-implicit conservative scheme. Let $[0, 1]$ be divided into N uniform cells such that $\Delta x = 1/N$, and let S_i^n satisfy:

$$S_i^{n+1} + \frac{\Delta t}{\Delta x} [F^I(S_{i+1}, S_i) - F^I(S_i, S_{i-1})] = S_i^n - \frac{\Delta t}{\Delta x} [F^E(S_{i+1}, S_i) - F^E(S_i, S_{i-1})], \quad (17)$$

for $i = 1, \dots, N$ and $n = 0, 1, \dots$. Here, $S_i^0 = 0$, $\Delta t = t^{n+1} - t^n$ is the time step, $S_i = S_i(t)$ is an approximate average value to the exact solution over grid-cell i at time-level t , and $S_i^n = S_i(t^n)$. The numerical flux is divided into an implicit and explicit part such that:

$$F^I(S_{i+1}, S_i) = -a_{i+1/2}^n \left(\epsilon b_{i+1/2}^n + \frac{\nu}{\Delta t} \right) \frac{S_{i+1}^{n+1} - S_i^{n+1}}{\Delta x},$$

$$F^E(S_{i+1}, S_i) = f_w(S_i^n) + a_{i+1/2}^n \frac{\nu}{\Delta t} \frac{S_{i+1}^n - S_i^n}{\Delta x},$$

with $a_{i+1/2}^n = (a(S_{i+1}^n) + a(S_i^n))/2$ and $b_{i+1/2}^n = (b(S_{i+1}^n) + b(S_i^n))/2$. Note that when $\epsilon = \nu = 0$, (17) reduces to the standard first order Godunov scheme since $f'(u) \geq 0$. This implies that the standard CFL-constraint on the time step must be imposed. In the calculations we choose $\Delta t = \Delta x / (2 \max_u f'(u))$.

3.1. Test case and numerical results

The non-dimensional form of the saturation equation allows us to test the effect of the dynamic capillary term for a wide range of characteristic values. Experimental results suggest that over the scale of a core plug, L should be in the range $10^4 - 10^7 \text{ kg/ms}$, see [10]. We will choose $\epsilon \sim 10^{-1} - 10^{-3}$. Since the dynamic capillary term is supposedly a perturbation, we choose $\nu \sim \epsilon - 10^{-2}\epsilon$. These numbers are also consistent with typical characteristic values including the given values for L . Assume that $K = \tilde{K}$. We will introduce some simple analytic forms for the constitutive relationships which will mimic

typical behavior of measured relationships. Assume that $k_{rw}(s) = \tilde{k}_w s^2$ and $k_{rn}(s) = \tilde{k}_n(1-s)^2$, then:

$$f_w(s) = \frac{s^2}{s^2 + \kappa(1-s)^2}, \quad a(s) = \frac{\kappa s^p(1-s)^p}{s^p + \kappa(1-s)^p}, \quad \text{and} \quad a(s)b(s) = 4s(1-s).$$

The last relationship captures the degeneracy of the product of the mobilities and the derivative at the residual saturations. In the computations we have chosen the mobility ratio to be $\kappa = 1$. Initially we assume that only the non-wetting phase is present $s_0(x) = 0$, and we impose a fixed flow rate of the wetting fluid at the inflow boundary, $u_w = \tilde{u}$, and a zero-Neumann condition at the outflow boundary:

$$f_w(s) - a(s)\left[\epsilon b(s)\frac{\partial s}{\partial x} + \nu\frac{\partial^2 s}{\partial x \partial t}\right] = 1 \quad \text{at} \quad x = 0, \quad \text{and} \quad \frac{\partial s}{\partial x} = 0 \quad \text{at} \quad x = 1. \quad (18)$$

These boundary conditions can be implemented using

$$F^I(S_1, S_0) + F^E(S_1, S_0) = 1, \quad \text{and} \quad S_{N+1}^n = S_N^n. \quad (19)$$

All the simulations were run to $t = 0.5$, equivalent to displacing half the effective pore-volume. To verify the implementation we checked that the solutions converged to the Buckley-Leverett profile in the limit $L, \epsilon \rightarrow 0$. We also checked the convergence rate in a discrete L_1 -norm defined by $\|f\|_1 = \sum_N |f_i| \Delta x_i$, by comparing a fine-grid solution, $N = 4000$, with coarse-grid solutions. The result is reported in Table 1, and suggests a convergence rate p close to 0.8. To investigate the effect of the dynamic term we ran

Table 1

Estimated L_1 -errors for $\epsilon = 0.01$ and different mesh parameters N at $t = 0.5$. The reference solution is computed with $N = 4000$ and p is the estimated order of convergence.

$N \setminus \nu$	0.01	0.001
25	0.1214	0.0550
50	0.0800	0.0385
100	0.0468	0.0258
200	0.0267	0.0152
400	0.0154	0.0077
800	0.0085	0.0034
p	0.7749	0.7986

simulations with various values for ϵ and L on a fine grid ($N = 4000$), and then calculated the redistribution of saturation in comparison to the Buckley-Leverett profiles $s = s^0(x, t)$ ($\epsilon = L = 0$), and the capillary diffusion solutions $s = s^\epsilon(x, t)$ ($L = 0$), at time $t = 0.5$. To measure the redistribution we used $D_0 = \|s - s^0\|_1 / \|s^0\|_1$ and $D_\epsilon = \|s - s^\epsilon\|_1 / \|s^\epsilon\|_1$. The results are reported in Table 2, and the saturation profiles for $\epsilon = 0.01$ and various values for L are shown in Figure 1. Qualitatively similar results to the profiles in Figure 1 were obtained for other choices of ϵ .

Table 2
 Redistribution of saturations: $N = 4000$, $t = 0.5$.

$\nu \setminus \epsilon$	D_0			D_ϵ		
	0.1	0.01	0.001	0.1	0.01	0.001
10^{-1}	0.1235	-	-	0.134	-	-
10^{-2}	0.2296	0.2261	-	0.0143	0.2590	-
10^{-3}	0.2595	0.0290	0.2868	0.0013	0.0567	0.2915
10^{-4}	-	-	0.2123	-	-	0.2172
10^{-5}	-	-	0.0128	-	-	0.0180
0	0.2438	0.0515	0.0086	0	0	0

4. DISCUSSION AND CONCLUSIONS

The results presented above suggest that the effect of a dynamic term may easily be of the same order as the effect of the equilibrium capillary pressure. We also observe significant effects of these terms on the mass distribution even for fairly small values of ϵ . Capillary effects are often neglected in standard petroleum applications because ϵ vanishes in the limit of high flow rates. However, the scaling of the dynamic term is independent of the characteristic flow rate. This may indicate that dynamic effects are important even in cases when capillary effects would normally be omitted.

The main effect of the dynamic term on the solution profiles is to retard the fronts. Since the simulations presented here are run with a fixed flow rate it follows that more mass accumulate behind the front and the front height is increased. A retardation effect was also observed for solutions of the Richards equation, see [10]. However, since the simulations reported in [10] were run with Dirichlet boundary conditions, no significant change of the shape of the fronts was observed, although the retardation was more pronounced.

Finally, to our knowledge no experiments have so far demonstrated that dynamic capillary terms may affect field scale displacement. Although numerical simulations, as presented in this and other work, may indicate the importance of such terms, experimental evidence in this direction is strongly needed.

REFERENCES

1. T. B. Benjamin, J. L. Bona and J. J. Mahony, Model equations for long waves in nonlinear dispersive systems. *Philos. Trans. Roy. Soc. London Ser. A* 272 (1972), no. 1220, 47–78.
2. J. L. Bona, W. R. McKinney, and J. M. Restrepo, Stable and unstable solitary-wave solutions of the generalized regularized long-wave equation. *J. Nonlinear Sci.* 10 (2000), no. 6, 603–638.
3. Z. Chen and R.E. Ewing, Comparison of Various Formulations of Three-Phase Flow in Porous Media, *J. Comp. Phys.*, (1997) 132.
4. G. Chavent and J. Jaffre, *Mathematical models and finite elements for reservoir simulation*, North Holland, Amsterdam (1996).
5. H.K. Dahle and M.A. Celia, A dynamic network model for two-phase immiscible flow,

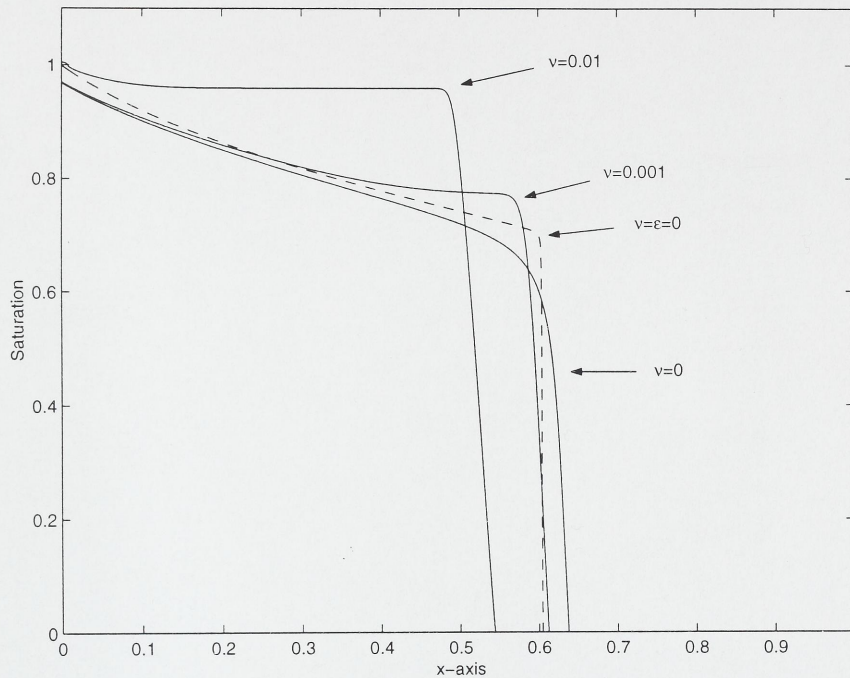


Figure 1. Solution profiles for various ν , $\epsilon = 0.01$, $N = 4000$, $t = 0.5$.

- Comp. Geosc., (1999) 3.
6. R. E. Ewing, Time-stepping Galerkin methods for nonlinear Sobolev partial differential equations. *SIAM J. Numer. Anal.* 15 (1978), no. 6, 1125–1150.
 7. W.G. Gray and S.M. Hassanizadeh, "Unsaturated flow theory including interfacial phenomena," *Water Resour. Res.*, (1991), 27, 1855-1863, 1991.
 8. S.M. Hassanizadeh and W.G. Gray, "Mechanics and thermodynamics of multiphase flow in porous media including interphase boundaries," *Adv. Water Resour.*, (1990), 13, 169-186.
 9. H. Gu, Characteristic finite element methods for nonlinear Sobolev equations. *Appl. Math. Comput.* 102 (1999), no. 1, 51–62.
 10. S.M. Hassanizadeh, M.A. Celia and H.K. Dahle, Dynamic effects in the capillary pressure-saturation relationship and their impacts on unsaturated flow, Submitted to the first issue of the *Vadose Zone Journal*, 2001
 11. J. Hulshof and J. R. King, Analysis of a Darcy flow model with a dynamic pressure saturation relation. (English. English summary) *SIAM J. Appl. Math.* 59 (1999), no. 1, 318–346 (electronic).
 12. B. Lucier, On nonlocal monotone difference schemes for scalar conservation laws. *Math. Comp.* 47 (1986), no. 175, 19–36.
 13. R. E. Showalter, Hilbert space methods for partial differential equations. *Monographs and Studies in Mathematics*, Vol. 1. Pitman, London-San Francisco, Calif.-Melbourne, 1977.



Depotbiblioteket



02sd 06 803

